

Dynamical Viability Assessment for Habitable Worlds Observatory Targets

STEPHEN R. KANE,¹ ZHEXING LI,¹ MARGARET C. TURNBULL,² COURTNEY D. DRESSING,³ AND CALEB K. HARADA^{3,*}

¹*Department of Earth and Planetary Sciences, University of California, Riverside, CA 92521, USA*

²*SETI Institute, Carl Sagan Center for the Study of Life in the Universe, Off-Site: 2613 Waunona Way, Madison, WI 53713, USA*

³*Department of Astronomy, 501 Campbell Hall #3411, University of California, Berkeley, CA 94720, USA*

ABSTRACT

Exoplanetary science is increasingly prioritizing efforts toward direct imaging of planetary systems, with emphasis on those that may enable the detection and characterization of potentially habitable exoplanets. The recent 2020 Astronomy and Astrophysics decadal survey recommended the development of a space-based direct imaging mission that has subsequently been referred to as the Habitable Worlds Observatory (HWO). A fundamental challenge in the preparatory work for the HWO search for exo-Earths is the selection of suitable stellar targets. Much of the prior efforts regarding the HWO targets has occurred within the context of exoplanet surveys that have characterized the stellar properties for the nearest stars. The preliminary input catalog for HWO consists of 164 stars, of which 30 are known exoplanet hosts to 70 planets. Here, we provide a dynamical analysis for these 30 systems, injecting a terrestrial planet mass into the Habitable Zone (HZ) and determining the constraints on stable orbit locations due to the influence of the known planets. For each system, we calculate the percentage of the HZ that is dynamically viable for the potential presence of a terrestrial planet, providing an additional metric for inclusion of the stars within the HWO target list. Our analysis shows that, for 11 of the systems, less than 50% of the HZ is dynamically viable, primarily due to the presence of giant planets whose orbits pass near or through the HZ. These results demonstrate the impact that known system architectures can have on direct imaging target selection and overall system habitability.

Keywords: astrobiology – planetary systems – planets and satellites: dynamical evolution and stability

1. INTRODUCTION

Although thousands of exoplanets have now been discovered, a full census and exploration of nearby planetary systems has yet to be realized. One of the primary reasons for incompleteness regarding nearby planetary architectures are the observational biases inherent within the two detection techniques responsible for the vast majority of current exoplanet discoveries: the radial velocity (RV) and transit methods (Cumming et al. 2008; Kane & von Braun 2008; Ford 2014; Winn & Fabrycky 2015; Kipping & Sandford 2016; He et al. 2019). Both of these methods are heavily biased toward large, close-in planets, with strong dependencies on survey design, data precision, observing strategy, and the time

baseline of observations (Kane et al. 2007; Ford 2008; von Braun et al. 2009; Wittenmyer et al. 2013; Barclay et al. 2018). However, RV surveys that have been operating for multiple decades have been able to probe beyond the snowline, providing insight into the prevalence of giant planets, even at relatively large separations from the host star (Wittenmyer et al. 2020; Fulton et al. 2021; Rosenthal et al. 2021). The architectures of these systems are informative for their orbital dynamics and evolution, that can also be used to constrain the possible presence of additional planets within those systems (Barnes & Raymond 2004; Kopparapu & Barnes 2010; Kane 2015; Kane & Blunt 2019; Kane 2023; Kane & Fetherolf 2023). Of particular interest is the potential for harboring planets within the Habitable Zone (HZ) of the system (Kasting et al. 1993; Kane & Gelino 2012; Kopparapu et al. 2013; Kane 2014; Kopparapu et al. 2014; Kane et al. 2016; Hill et al. 2018; Kane et al. 2020a; Hill et al. 2023). Such HZ planets are expected to be

skane@ucr.edu

* NSF Graduate Research Fellow

the target of extensive follow-up observations, especially those nearby systems whose host star brightness and angular separation of their planets may enable direct imaging as a means to characterize the planetary atmospheres (Brown 2015; Barclay et al. 2017; Kane et al. 2018; Kopparapu et al. 2018; Stark et al. 2020; Li et al. 2021).

Among the recommendations of the 2020 Astronomy and Astrophysics decadal survey (hereafter Astro2020) was the prioritization of a space-based mission with the capability to directly image terrestrial planets within the HZ¹. The currently adopted name for this recommended mission is the Habitable Worlds Observatory (HWO), and considerable efforts are being undertaken to define the mission designs that would maximize the science yield for terrestrial planet characterization (Vaughan et al. 2023; Stark et al. 2024). Work is also being carried out to both define and characterize the target stars that are best suited for HWO observations. An initial list of 164 HWO target stars has been provided to the broader community for assessment and discussion (Mamajek & Stapelfeldt 2024), the stellar properties of which have been further refined by Harada et al. (2024) and examined in the context of yield simulations by Tchow et al. (2024). Of these 164 nearby stars, all of which lie within 24 pcs, 30 are currently known to host exoplanets, with a total inventory of 70 known exoplanets. These exoplanet detections have primarily been enabled through long-term RV observations, revealing the Keplerian orbits and architectures down to the RV precision of the corresponding surveys. Though the architectures for these planetary systems are likely incomplete, even partial knowledge of the planets present enables a dynamical analysis that can inform the likelihood that each system has a HZ that contains dynamically viable orbital locations for terrestrial planets. Given the need to determine a high quality list of HWO targets, deprioritizing those systems that are dynamically unsuitable is a crucial step in the target assessment process.

In this work, we present the results of a dynamical study for the known exoplanet hosts within the current proposed HWO target list provided by Mamajek & Stapelfeldt (2024), that specifically provides an assessment for the dynamical stability within the HZ of those systems. Section 2 provides a description of the HWO stellar sample, with a particular emphasis on the known exoplanetary systems within that list. The description includes a tabulation of the stellar and plan-

etary properties for the known exoplanet systems, and the methodology for the calculation of the system HZ boundaries. The structure and results from the dynamical simulations are described in Section 3, with a quantification of the available HZ that is dynamically stable. We discuss the implications and limitations of our work in Section 4, and provide concluding remarks and suggestions for future work in Section 5.

2. THE HABITABLE WORLDS OBSERVATORY SAMPLE

Here, we provide the details of the potential HWO target list that harbor known exoplanets, and discuss the calculation of the HZ for these systems.

2.1. *Known Planetary Systems*

From the 164 stars identified by Mamajek & Stapelfeldt (2024), we extracted the 30 stars that are currently known to host exoplanets (Akeson et al. 2013). The full list of planets for all of the included systems, including their relevant stellar and planetary properties, are provided in Table 1. The selection of relevant parameters means those that are needed for the calculation of the HZ and/or the dynamical simulations, described in Section 3. Note that the HH Peg (HD 206860) system was not included in our analysis since the companion is a brown dwarf at very wide separation from the host star, detected using the direct imaging technique (Luhman et al. 2007). The sources for the stellar/planetary parameters used in all cases are included in the final column of Table 1, where the source selection is based upon the most complete data source.

The stellar multiplicity of a planetary system can have a significant dynamical effect on HZ planets (Holman & Wiegert 1999; Kane & Hinkel 2013; Simonetti et al. 2020). Of the 30 known exoplanet hosts in our sample, 9 of the stars are known to have stellar or brown dwarf companions. The HD 3651 system has a brown dwarf with a projected separation of 476 AU away the primary (Luhman et al. 2007). The HD 9826 system contains a red dwarf star with a projected separation of 750 AU from the primary (Mason et al. 2001). HD 26965 is a triple system, whereby the B and C components are a white dwarf and red dwarf star, respectively, and orbit each other at a distance of ~ 400 AU from the primary (Bond et al. 2017). The HD 75732 system contains a red dwarf star with a projected separation of 1100 AU from the primary (Marcy et al. 2002). The HD 102365 includes a red dwarf star with a projected separation of 211 AU from the primary (Raghavan et al. 2010). HD 115404A is in a binary orbit with a red dwarf star that has projected separation of 289 AU (Alonso-Floriano et al. 2015). HD 147513 is in a binary orbit

¹ <https://www.nationalacademies.org/our-work/decadal-survey-on-astronomy-and-astrophysics-2020-astro2020>

with a white dwarf separated by ~ 5300 AU (Porto de Mello & da Silva 1997). The HD 190360 system includes a red dwarf star that is separated by at least 1266 AU from the primary (Naef et al. 2003) and is probably at a much larger distance (Feng et al. 2021). The HD 209100 system contains a brown dwarf binary pair that is separated from the primary by 1500 AU (Scholz et al. 2003; Luhman et al. 2007; King et al. 2010). Given the wide separations for all of these binary/multiple systems, and the considerable uncertainties in their orbital parameters, the stellar or brown dwarf companions were not included in our subsequent dynamical analysis.

There are several further important notes regarding the included systems. The vast majority of the 70 planets are not known to transit their host star, and so the planetary masses used are minimum masses in most cases, the implications of which are discussed in Section 4. Exceptions to this include HD 39091 c (Huang et al. 2018), HD 75732 e (Demory et al. 2011; Kane et al. 2011; von Braun et al. 2011; Winn et al. 2011), HD 136352 b, c, and d (Kane et al. 2020b; Delrez et al. 2021), and HD 219134 b and c (Gillon et al. 2017), all of which are known to transit their host stars. There are also planets in our list for which orbital inclination measurements have been made. For HD 39091, planet b has an inclination of $\sim 50^\circ$, resulting in a mutual inclination of $\sim 40^\circ$ with respect to planet c (Xuan & Wyatt 2020), and we assume planet d is coplanar with planet b. For HD 115404A, planet c has an inclination of $\sim 25^\circ$, and we assume planet b is coplanar (Feng et al. 2022). For HD 140901, planet c has an inclination of $\sim 170^\circ$, and we assume planet b is coplanar (Feng et al. 2022). For HD 160691, astrometry places an upper limit on the inclination of $\sim 60^\circ$ for the known planets (Benedict et al. 2022). For HD 209100 b, Feng et al. (2019) provides an inclination of $\sim 64^\circ$, thus establishing the actual planetary mass. Planet masses reported in the literature as Earth mass units (M_\oplus) have been converted to Jupiter mass units (M_J) in Table 1 for consistency. For cases where the eccentricity is reported as zero, the argument of periastron is set to 90° , corresponding to the location of inferior conjunction. Finally, note that the existence of the planet orbiting HD 26965 (Ma et al. 2018) has been disputed from RV follow-up data (Burrows et al. 2024), but we elected to err on the side of caution and included the planet in our list.

The exoplanet population included in our sample is represented in Figure 1, showing the distributions of semi-major axes and eccentricities. The ranges of these values within the sample are 0.015–11.6 AU and 0.0–0.64 for the semi-major axes and eccentricities, respectively. The data point sizes are logarithmically propor-

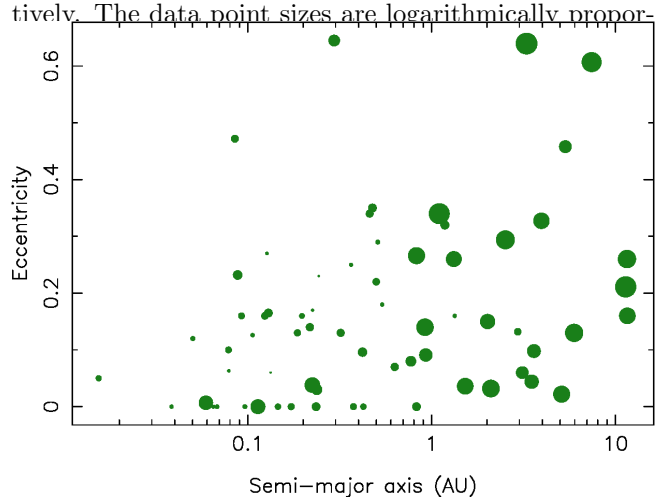


Figure 1. Distribution of semi-major axes and eccentricities for all planets included in our sample. The size of the plotted data are logarithmically proportional to the planet mass.

tional to the planet mass, with a range of $0.0055 M_J$ (tau Ceti g) to $12.6 M_J$ (pi Men b). There are several features to consider regarding the parameter distribution shown in Figure 1. There is a clear trend toward higher mass planets at larger separations. For example, the mean planet mass for semi-major axes less than 1 AU is $0.19 M_J$, whereas the mean planet mass beyond 1 AU is $1.19 M_J$. A significant factor in this planetary mass trend is the observational bias inherent in the RV method, whereby the RV amplitude decreases with increasing semi-major axis (Cumming 2004; O’Toole et al. 2009). A similar bias impacts the observed eccentricity distribution, since such planets produce higher RV amplitudes, albeit during a limited period of the orbital phase (Kane et al. 2007; Shen & Turner 2008; Zakamska et al. 2011; Kane et al. 2012). Moreover, for those long-period planets with insufficient phase coverage, the relatively slow apastron passage may result in eccentricity misclassifications (Anglada-Escudé et al. 2010; Hara et al. 2019; Wittenmyer et al. 2019a). Even so, the combination of relatively high masses and eccentricities produces numerous planetary architectures that exhibit significant dynamical consequences within the HZ of their systems.

Table 1. Stellar and planetary parameters for HWO known systems.

Star	NP^\dagger	M_\star (M_\odot)	T_{eff} (K)	Planet	M_p^\ddagger (M_J)	a (AU)	e	ω ($^\circ$)	Source
HD 3651 (54 Piscium)	1	0.799	5221	b	0.228	0.295	0.645	243	Wittenmyer et al. (2019b)
HD 9826 (ups And)	3	1.29	6156	b	0.675	0.05914	0.0069	0	Rosenthal et al. (2021)
				c	1.965	0.8265	0.266	58.2	
				d	4.1	2.517	0.294	73.8	
HD 10647 (q1 Eridani)	1	1.11	6218	b	0.94	2.015	0.15	212	Marmier et al. (2013)
HD 10700 (tau Ceti)	4	0.78	5333	g	0.0055	0.133	0.06	395.34	Feng et al. (2017b)
				h	0.0058	0.243	0.23	7.45	
				e	0.0124	0.538	0.18	22.35	
				f	0.0124	1.334	0.16	119.75	
HD 17051 (iota Hor)	1	1.34	6167	b	2.27	0.92	0.14	309	Stassun et al. (2017)
HD 20794 (82 Eridani)	4	0.813	5401	b	0.0089	0.127	0.27	386.17	Feng et al. (2017a)
				c	0.0079	0.225	0.17	31.51	
				d	0.0111	0.364	0.25	252.67	
				e	0.015	0.509	0.29	268.14	
HD 22049 (eps Eri)	1	0.81	5020	b	0.651	3.5	0.044	350	Rosenthal et al. (2021)
HD 26965 (40 Eri)	1	0.78	5072	b	0.0267	0.219	0.04	148.969	Ma et al. (2018)
HD 33564 (kappa Cam)	1	1.25	6250	b	9.1	1.1	0.34	205	Galland et al. (2005)
HD 39091 (pi Men)	3	1.07	5998	c	0.0114	0.06805	0	90	Hatzes et al. (2022)
				d	0.0421	0.499	0.22	323	
				b	12.6	3.2826	0.6396	331.03	
HD 69830	3	0.86	5385	b	0.0321	0.0785	0.1	340	Lovis et al. (2006)
				c	0.0371	0.186	0.13	221	
				d	0.057	0.63	0.07	224	
HD 75732 (55 Cancri)	5	0.905	5172	e	0.0251	0.01544	0.05	86	Bourrier et al. (2018)
				b	0.8036	0.1134	0	90	
				c	0.1611	0.2373	0.03	2.4	
				f	0.1503	0.7708	0.08	262.4	
				d	3.12	5.957	0.13	290.9	
HD 95128 (47 UMa)	3	1.06	5872	b	2.53	2.1	0.032	334	Gregory & Fischer (2010)
				c	0.54	3.6	0.098	295	
				d	1.64	11.6	0.16	110	
HD 95735	2	0.3899	3712	b	0.0085	0.07879	0.063	330	Hurt et al. (2022)
				c	0.0428	2.94	0.132	63	
HD 102365	1	0.85	5630	b	0.0503	0.46	0.34	105	Tinney et al. (2011)
HD 114613	1	1.27	5641	b	0.357	5.34	0.458	196	Luhn et al. (2019)
HD 115404A	2	0.83	5019	b	0.097	0.088	0.232	259	Feng et al. (2022)
				c	10.319	11.364	0.211	312	
HD 115617 (61 Vir)	3	0.942	5577	b	0.016	0.050201	0.12	105	Vogt et al. (2010)
				c	0.057	0.2175	0.14	341	

Table 1 continued

Table 1 (*continued*)

Star	NP^\dagger	M_\star (M_\odot)	T_{eff} (K)	Planet	M_p^\ddagger (M_J)	a (AU)	e	ω ($^\circ$)	Source
				d	0.072	0.476	0.35	314	
HD 136352 (nu2 Lupi)	3	0.87	5664	b	0.0149	0.0964	0	90	Delrez et al. (2021)
				c	0.0354	0.1721	0	90	
				d	0.0278	0.425	0	90	
HD 141004 (lambda Ser)	1	1.05	5885	b	0.0428	0.1238	0.16	19.48	Rosenthal et al. (2021)
HD 140901	2	0.99	5586	b	0.0503	0.085	0.472	108	Feng et al. (2022)
				c	6.284	7.421	0.607	298	
HD 143761 (rho CrB)	4	0.95	5817	e	0.0119	0.1061	0.126	359.4	Brewer et al. (2023)
				b	1.093	0.2245	0.038	269.64	
				c	0.0887	0.4206	0.096	9.7	
				d	0.068	0.827	0	90	
HD 147513 (62 G. Sco)	1	1.11	5883	b	1.21	1.32	0.26	282	Mayor et al. (2004)
HD 160691 (mu Ara)	4	1.13	5773	d	0.033	0.0923	0.16	197	Benedict et al. (2022)
				e	0.439	0.9296	0.091	193	
				b	1.665	1.5224	0.036	39	
				c	1.873	5.0937	0.022	84	
HD 189567	2	0.83	5726	b	0.0267	0.111	0	90	Unger et al. (2021)
				c	0.022	0.197	0.16	219	
HD 190360	2	0.99	5537	c	0.0677	0.1294	0.165	322	Rosenthal et al. (2021)
				b	1.492	3.955	0.3274	13.9	
HD 192310	2	0.8	5166	b	0.0532	0.32	0.13	173	Pepe et al. (2011)
				c	0.076	1.18	0.32	110	
HD 209100 (eps Indi A)	1	0.754	4611	b	3.25	11.55	0.26	77.83	Feng et al. (2019)
HD 217987	2	0.489	3688	b	0.0132	0.068	0	90	Jeffers et al. (2020)
				c	0.0239	0.12	0	90	
HD 219134	6	0.794	4913	b	0.012	0.038474	0	90	Vogt et al. (2015)
				c	0.011	0.064816	0	90	
				f	0.028	0.14574	0	90	
				d	0.067	0.23508	0	90	
				g	0.0346	0.3753	0	90	
				h	0.34	3.11	0.06	215	

[†]Number of planets.

[‡]Minimum mass, except for 55 Cancri e and the HD 136352 planets.

2.2. System Habitable Zones

The extent of the HZ for each system was calculated using the stellar parameters from the sources provided in Table 1. Specifically, we adopt the methodology provided by Kopparapu et al. (2013, 2014), in which the

boundaries of the HZ are derived from 1D Earth-based climate models that calculate the radiative balance for which surface liquid water is retained. This approach divides the HZ into two primary regions: the conservative HZ (CHZ) and the optimistic HZ (OHZ). The CHZ is bounded by the runaway greenhouse criteria at the inner edge, and the maximum CO₂ greenhouse criteria at the outer edge (Kane et al. 2016). The OHZ is an empirical

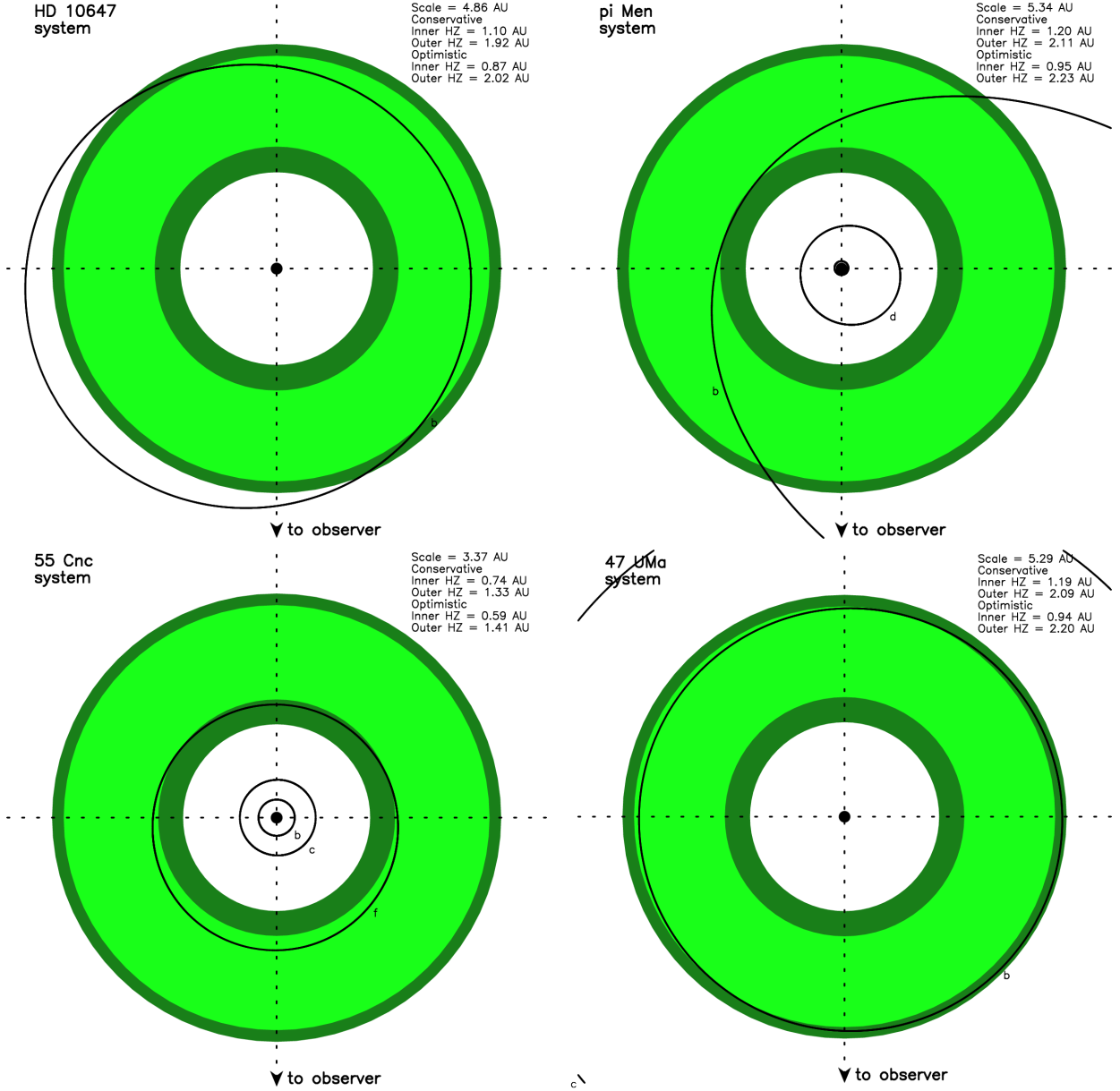


Figure 2. HZ and planetary orbits for four of the systems in our sample: HD 10647 (top-left), HD 39091 (pi Men; top-right), HD 75732 (55 Cancri; bottom-left), HD 95128 (47 Uma; bottom-right). The orbits are labeled by planet designation. The extent of the HZ is shown in green, where light green and dark green indicate the CHZ and OHZ, respectively.

extension to the CHZ based upon assumptions regarding retention of surface liquid water in the Venusian and Martian evolutionary histories (Baker 2001; Kane et al. 2014; Way et al. 2016; Orosei et al. 2018; Kane et al. 2019; Kane & Byrne 2024). The CHZ and OHZ boundaries for each system are provided in Table 2.

Figure 2 and Figure 3 show top-down views for 8 of the planetary systems, that demonstrate the diversity of architectures in our known exoplanet host sample. The extent of the CHZ and OHZ are shown in light green and dark green, respectively. In most of these cases, the

planetary orbit that is present within the HZ is a giant planet with significant perturbation potential. The cases where eccentric orbits lie within and/or cross the HZ, such as HD 39091 (pi Men), HD 114613, HD 147513, and HD 192310, are particularly devastating to orbital stability in that region due to angular momentum transfer that excites other planetary orbits into high eccentricity regimes (Kane & Raymond 2014). The others cases shown exhibit planetary orbits that are more circular, and can often allow regions of orbital stability at the edges of the HZ. These scenarios may be tested

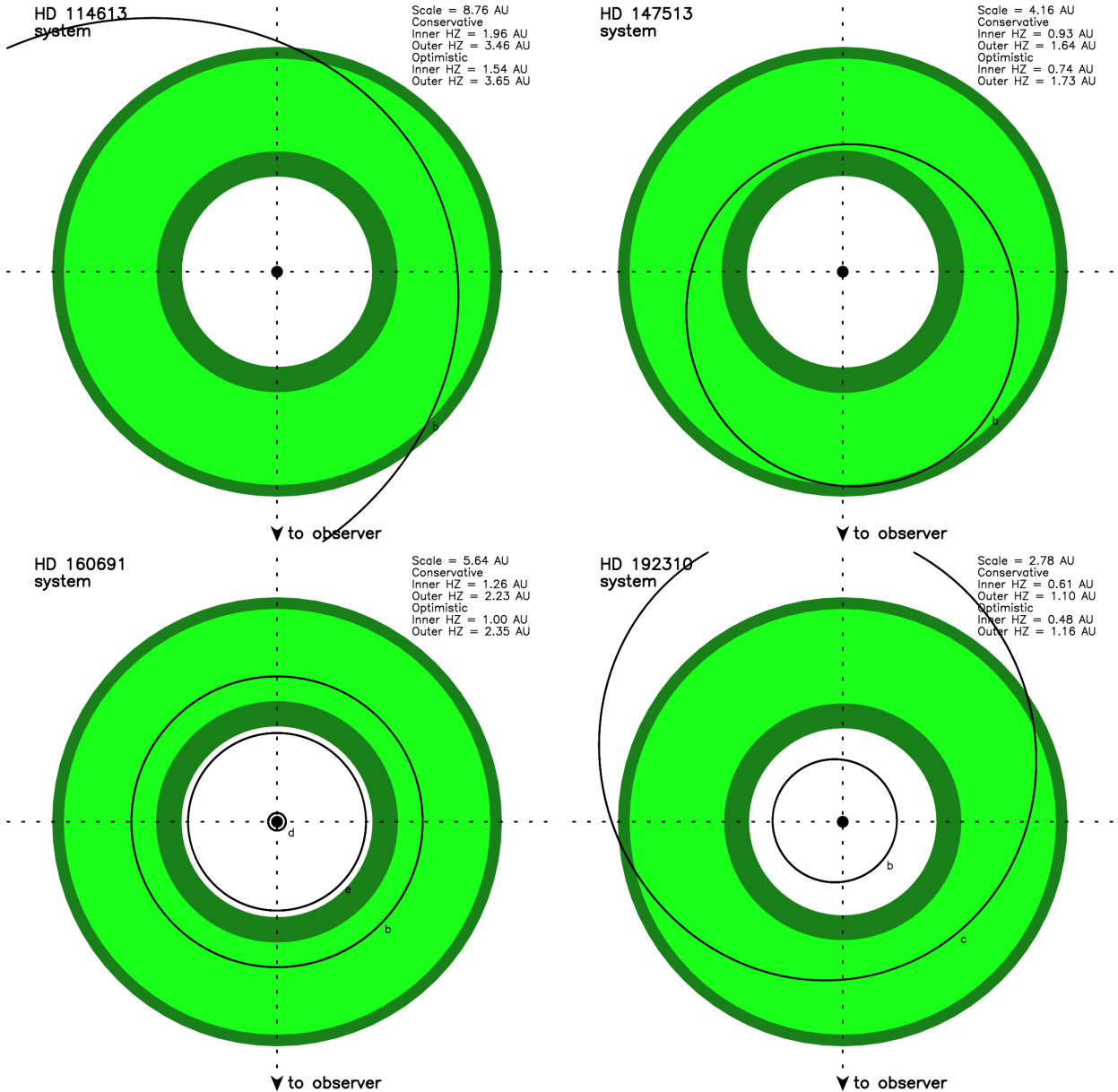


Figure 3. HZ and planetary orbits for four of the systems in our sample: HD 114613 (top-left), HD 147513 (top-right), HD 160691 (bottom-left), HD 192310 (bottom-right). The orbits are labeled by planet designation. The extent of the HZ is shown in green, where light green and dark green indicate the CHZ and OHZ, respectively.

with dynamical simulations that explore particle injection throughout the HZ region.

3. ORBITAL DYNAMICS

3.1. Simulation Design

We conducted an exhaustive series of dynamical simulations to test the viability of terrestrial planets orbiting within the HZ of the target systems. The simulations were conducted using the REBOUND N-body integrator package (Rein & Liu 2012) that applies the symplectic integrator WHFast (Rein & Tamayo 2015). Our

simulations explored the effect and orbital evolution of an additional Earth-mass planet in a circular orbit that is coplanar with the other planets within each system, where 10 equally spaced mean anomalies were chosen for the injected planet. For the case of HD 39091 (pi Men), where there is a substantial mutual inclination between the planets, we injected the additional planet in an orbit coplanar with planet b, since that is the planet that dominates the gravitational influence on the HZ for that system (see Section 2.1 and Figure 2). The semi-major axes explored spanned 20% less than the inner edge

of the OHZ to 20% larger than the outer edge of the OHZ (see Section 2.2). This region within each system was divided into 1000 equally spaced semi-major axis starting locations for the injected planet to ensure sufficiently dynamical sampling of the HZ. Each of these semi-major axis and mean anomaly starting locations were integrated for 10^7 years, resulting in 10,000 simulations performed for each system. The time step for each integration was selected based upon the orbital period for the innermost body within the system divided by 20, where the innermost body is either a known planet or the injected planet.

At each of the simulation starting locations, our simulations provided the percentage of the total simulation duration for which the planet was able to survive, where non-survival means that the injected planet was captured by the gravitational well of the host star or ejected from the system. From these results, we calculated the dynamically viable HZ (DVHZ), which is the percentage of the OHZ locations for which the injected planet survived the full 10^7 year simulation.

3.2. Habitable Zone Stability Results

The methodology described in Section 3.1 was applied to each of the systems shown in Table 1. The time required to complete the suite of simulations for each system varied enormously, depending upon the number of planets in the system, their locations, and the extent of the instability induced within the HZ. For example, the 55 Cancri system (bottom-left system depicted in Figure 2) contains 5 known planets, including one with a 0.74 day orbit, resulting in the need for high time resolution within the dynamical simulation. By contrast, systems with a single, eccentric giant planet with high scattering potential (such as the HD 147513 system) concluded the simulation suite relatively quickly.

The simulation results for 8 of the systems are represented in Figure 4 and Figure 5, corresponding to the same systems shown in Figure 2 and Figure 3, respectively. The plots provide the percentage of the full 10^7 year simulation for which the injected terrestrial planet was able to maintain a stable orbit for each semi-major axis location. As for Figure 2 and Figure 3, the CHZ and OHZ are shown as light green and dark green shaded regions, respectively. In all of the 8 cases shown, there are significant areas of instability within the HZ resulting from the known planets in the system. Most notable is the case of pi Men (second panel; Figure 4) in which the entire region explored is unstable due to the incursion of the highly eccentric b planet into the HZ. The HD 147513 system (second panel; Figure 5) is similarly affected, although stable regions exist just outside

of the HZ. The remaining examples shown have varying amounts of stable locations within the HZ, including regions of stability/instability resulting from a combination of mean motion resonance (MMR) effects and the numerical randomness intrinsic to the simulations (Raymond et al. 2008; Petrovich et al. 2013; Hadden 2019). For example, the results for HD 10647 (first panel; Figure 4) exhibits numerous stability islands induced by the single giant planet in the system. The 3:2 MMR location at 1.53 AU creates an island of stability whereby a planet located there has the potential to avoid gravitational perturbing interactions with the known giant planet, similar to the 2:3 MMR of Neptune with Pluto (Williams & Benson 1971). Of particular note is the 5:2 MMR location at 1.09 AU that produces a region of instability that coincides with the inner boundaries of the OHZ and CHZ. Multi-planet systems can exhibit significantly complicated stability patterns due to the multitude of MMR locations cascading throughout the system, as shown in the case of HD 75732 (55 Cancri; third panel; Figure 4).

To quantify the dynamical simulation results on a system-by-system basis, we calculate and provide the DVHZ in each case, as described in Section 3.1. These calculations are shown in Table 2, along with the inner and outer boundaries for the CHZ and OHZ, described in Section 2.2. For 11 of the systems, DVHZ is less than 50%, and there are 4 cases where the DVHZ is 0%, including the previously discussed systems of HD 39091 (pi Men) and HD 147513. In general, the architectures for the 11 cases where DVHZ is less than 50% are dominated by a giant planet in an eccentric orbit that passes near or through the HZ.

On the other hand, there are 9 cases for which the DVHZ is 100%. Cross-referencing these systems with Table 1 reveals that their architectures are dominated by low-mass, short-period planets with limited gravitational influence within the HZ. Shown in Figure 6 is a histogram of the DVHZ values that summarizes the findings of our dynamical simulations. This shows that half of the studied systems have DVHZ values that are greater than 80%, ensuring that there is substantial dynamically viable space within the HZ of those systems based on the currently known architectures, and therefore suitable for potential direct imaging follow-up observations.

4. DISCUSSION

Given the number of known exoplanetary systems, including those resulting from numerous decades of RV observations around bright stars, it is little surprise that

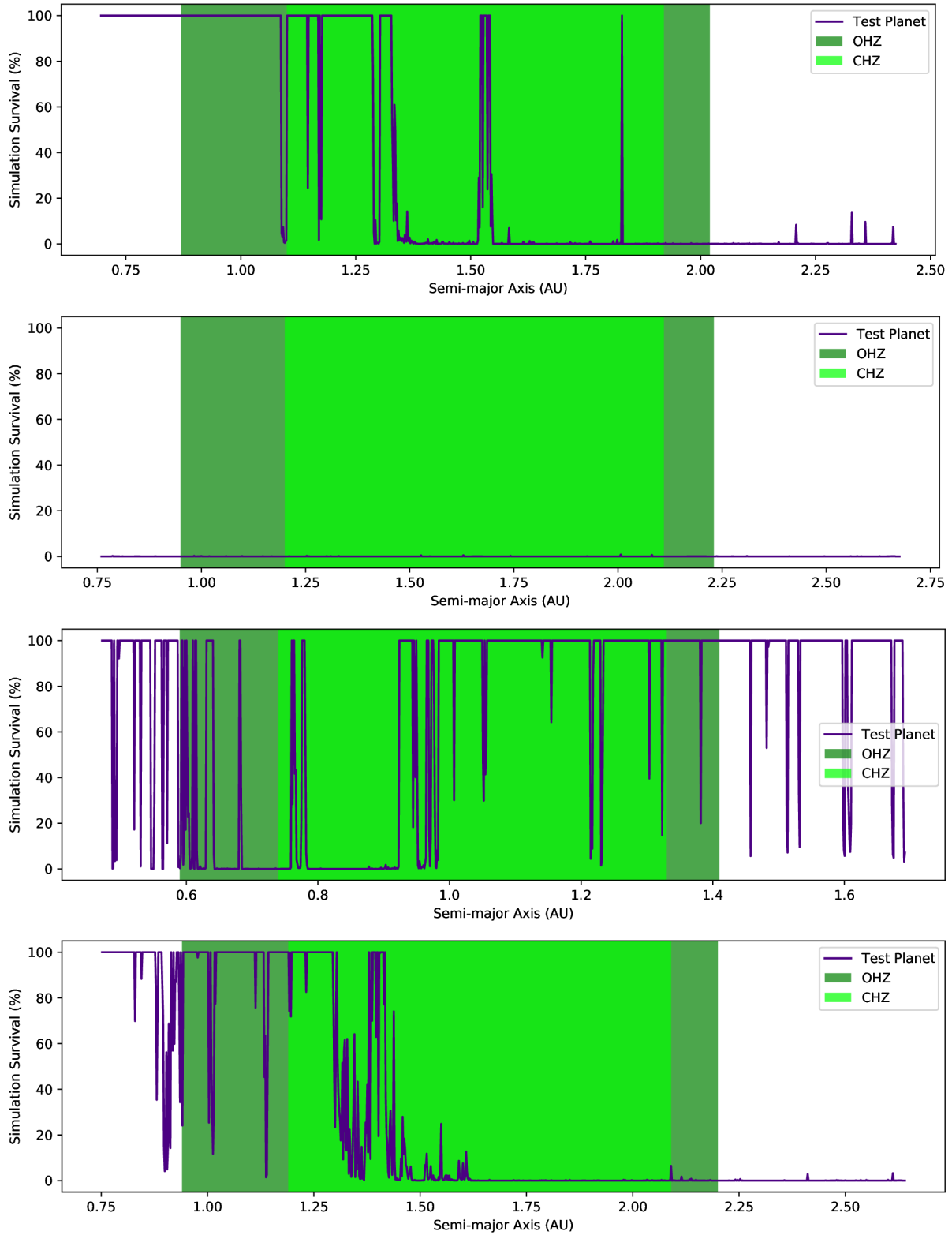


Figure 4. Percentage of the simulation that the injected Earth-mass planet survived as a function of the initial semi-major axis, where the CHZ is shown in light green and the OHZ is shown in dark green. Shown, from top to bottom, are the results for HD 10647, HD 39091 (pi Men), HD 75732 (55 Cancri), and HD 95128.

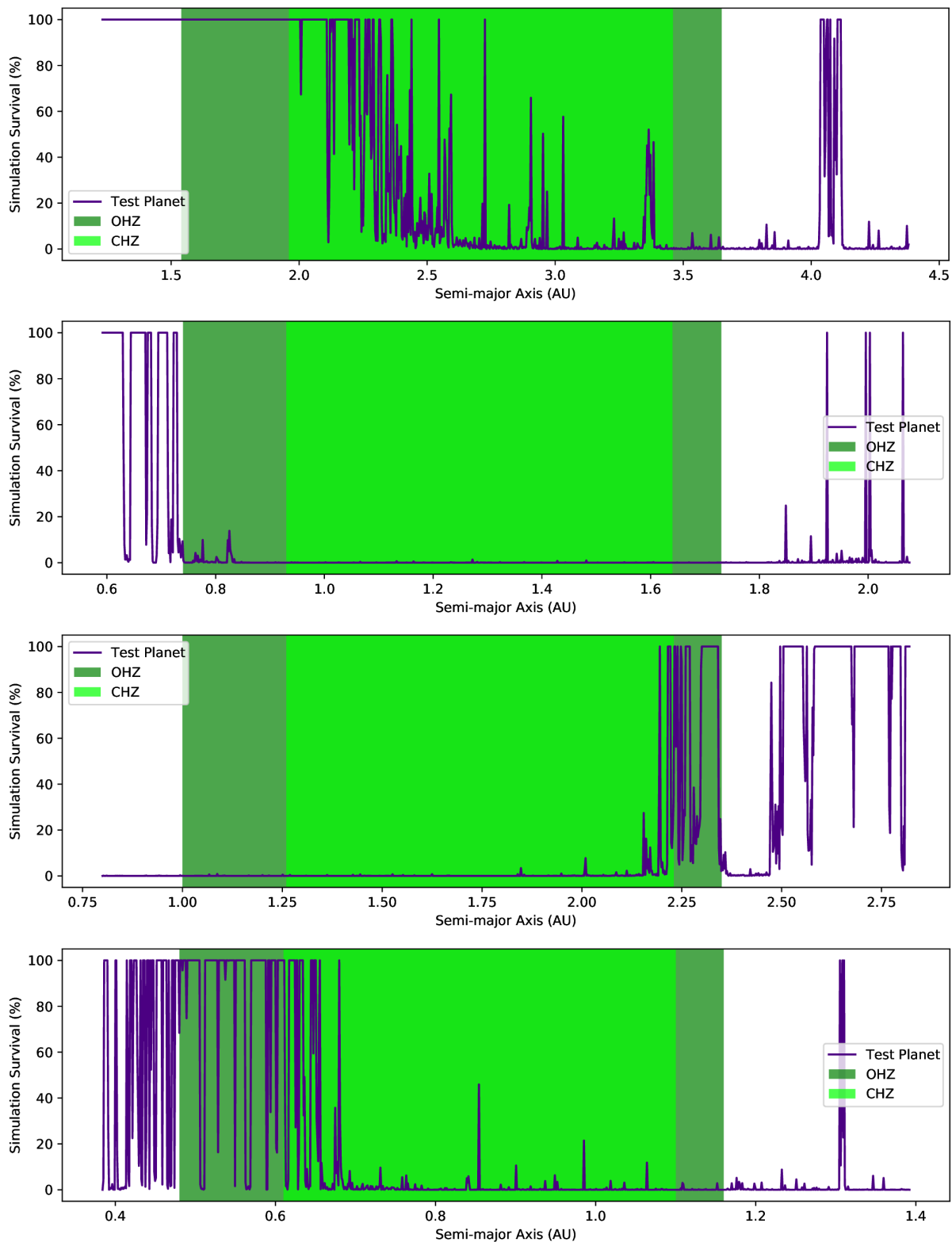
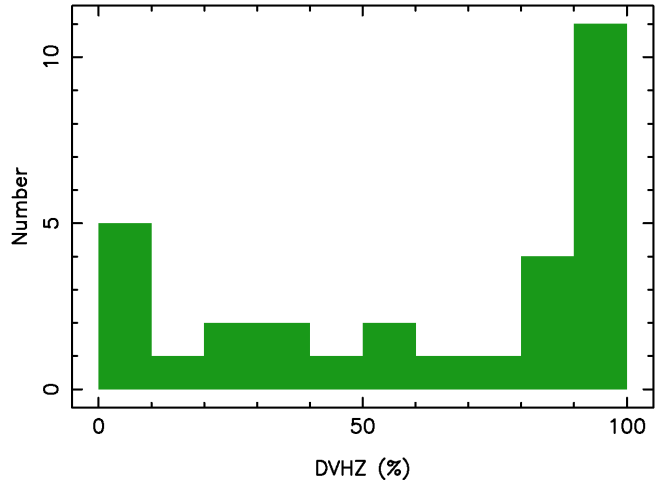


Figure 5. Percentage of the simulation that the injected Earth-mass planet survived as a function of the initial semi-major axis, where the CHZ is shown in light green and the OHZ is shown in dark green. Shown, from top to bottom, are the results for HD 114613, HD 147513, HD 160691, and HD 192310.

Table 2. HZ boundaries and DVHZ results.

Star	OHZ _{in} (AU)	CHZ _{in} (AU)	CHZ _{out} (AU)	OHZ _{out} (AU)	DVHZ (%)
HD 3651	0.56	0.71	1.27	1.34	92.41
HD 9826	1.35	1.71	3.00	3.16	0.00
HD 10647	0.87	1.10	1.92	2.02	38.65
HD 10700	0.55	0.69	1.24	1.31	20.75
HD 17051	0.94	1.20	2.09	2.20	55.02
HD 20794	0.72	0.91	1.63	1.72	0.00
HD 22049	0.45	0.57	1.03	1.09	100.00
HD 26965	0.52	0.66	1.20	1.26	100.00
HD 33564	1.58	2.00	3.49	3.68	61.50
HD 39091	0.95	1.20	2.11	2.23	0.00
HD 69830	0.60	0.75	1.35	1.42	84.48
HD 75732	0.59	0.74	1.33	1.41	56.99
HD 95128	0.94	1.19	2.09	2.20	27.59
HD 95735	0.13	0.16	0.30	0.32	100.00
HD 102365	0.57	0.72	1.28	1.35	78.21
HD 114613	1.54	1.96	3.46	3.65	33.43
HD 115404A	0.43	0.54	0.99	1.04	100.00
HD 115617	0.68	0.86	1.53	1.61	44.93
HD 136352	0.77	0.97	1.72	1.82	100.00
HD 140901	0.69	0.87	1.54	1.62	89.06
HD 141004	1.08	1.36	2.40	2.53	100.00
HD 143761	1.01	1.28	2.25	2.38	88.17
HD 147513	0.74	0.93	1.64	1.73	0.00
HD 160691	1.00	1.26	2.23	2.35	5.39
HD 189567	1.09	1.38	2.45	2.58	100.00
HD 190360	0.82	1.04	1.84	1.94	85.67
HD 192310	0.48	0.61	1.10	1.16	19.14
HD 209100	0.38	0.48	0.87	0.92	100.00
HD 217987	0.16	0.20	0.38	0.40	100.00
HD 219134	0.41	0.52	0.95	1.00	99.26

the HWO target list contains known exoplanet systems. The description of these 30 systems in Section 2 shows that the architectures of these systems is diverse, including low-mass multi-planet systems and high-mass single-planets in eccentric orbits. The latter category includes giant planets beyond the snow line, the frequency of which appears to be relatively rare (Albrow et al. 2001; Wittenmyer et al. 2011, 2016; Fulton et al. 2021; Rosenthal et al. 2021; Bonomo et al. 2023), and can greatly influence the volatile delivery within the system (Raymond & Bonser 2014; Raymond & Izidoro 2017; Venturini et al. 2020; Kane & Wittenmyer 2024). The high eccentricity cases may be the result of planet-planet

**Figure 6.** Histogram of the DVHZ calculations for all 30 of the known systems studied in this work.

scattering events (Carrera et al. 2019) and can dynamically eliminate the possibility of further planets being present in the system (Brewer et al. 2020). The growing understanding of such dynamically volatile systems, including their formation and prevalence, will greatly inform our ability to infer the possible presence of HZ exoplanets (Barnes & Raymond 2004).

As described in Section 3.1, the integration time for each of our simulations was 10^7 years. The integration time was chosen to minimize the effects of orbital element error propagation (Ford 2005; Kane et al. 2009), and to create a feasible pathway to explore the full parameter space for all 30 targets, each of which required thousands of simulations. However, chaotic systems are often the result of divergent orbital eccentricities that can require significant time to develop. It is thus possible that, even for locations identified as stable in our simulations, instability occurs beyond the 10^7 year integration time (Goździewski et al. 2001). Although our criteria for stability is a first-order approach that necessitates all planets survive the duration of the dynamical simulation, this criteria has successfully been validated against chaos indicators (Dvorak et al. 2010) and applied to numerous exoplanetary systems (Menou & Tabachnik 2003; Dvorak et al. 2003; Kane 2016).

As noted in Section 2.1, the preponderance of planets in our sample are not known to transit their host stars, whereby the true mass of the planet may be realized. Thus, the planetary masses used are generally minimum masses. A consequence of this knowledge limitation is that the dynamical influence of the planets on each other within a system, and their effects on the injected planet, may be larger than that calculated and presented here. For that reason, the results presented

in Section 3.2 can be considered a lower limit on the HZ orbital instability. Furthermore, the observational bias in the RV and transit methods mentioned in Section 2.1 means that the architectures of the known systems are likely incomplete, with additional planets yet to be discovered in these systems. However, it is worth repeating here that we assumed coplanar orbits for the injected planets in our simulations (coplanar with planet b in the case of pi Men). A full exploration of terrestrial HZ planets whose orbits are mutually inclined from the known planets may yet reveal stable locations that are otherwise unviable.

5. CONCLUSIONS

The effective transition of the exoplanet community to prioritizing direct imaging techniques requires that the data for the expected stellar targets be sufficiently leveraged toward a robust target list. Of the 164 targets provided by Mamajek & Stapelfeldt (2024) for direct imaging with HWO, only $\sim 20\%$ are presently known to harbor exoplanets. Most, if not all, of the remaining stars likely also have planetary companions, but in most cases the current database of RV observations may be sufficient to rule out the presence of giant planets in or near the HZ. For those that are known exoplanet hosts, our results show that 11 of the systems have less than 50% of the HZ that is dynamically viable ($DVHZ < 50\%$), including 4 cases where there is no dynamically possible orbit (ups And, eps Eri, pi Men, and 62 G. Sco). These systems should therefore be treated with extreme caution when considered as possible HWO targets. However, over half of the tested systems have DVHZ values greater than 80%, making them suitable HWO targets from the perspective of orbital dynamics. Moreover, our overall results are not necessarily representative of what may be expected for the broader list of HWO targets where no exoplanets have yet been detected. Giant planets are relatively rare among the exoplanet population, and the detection methods utilized are biased toward detecting those kinds of planets more quickly than lower-mass planetary counterparts. This means that current exoplanet surveys may have already detected many of

the nearby systems that contain significant perturbing agents (giant planets) for possible terrestrial HZ planets.

With respect to exoplanet architectures, the refinement of the HWO target sample will greatly benefit from the continued search for exoplanets. The era of extreme precision RVs (Fischer et al. 2016) provides opportunities to detect previously undiscovered exoplanets around the nearby stars. These exoplanet detections will include low-mass terrestrial exoplanets and high-mass planets with low-inclinations relative to the plane of the sky. Additional planets are also likely to be found in the known systems, further constraining the stability profiles for the HZ region, as described in this work. Results from the Gaia mission (Gaia Collaboration et al. 2021) will aid in the detection of long-period giant planets and allow the true mass of known RV giant planets to be determined. All of these precursor observational efforts will continue to form an essential component for the success of the Astro2020 recommendations, and maximize the yield of HWO and the characterization of HZ terrestrial planets.

ACKNOWLEDGEMENTS

We acknowledge support from the NASA Astrophysics Decadal Survey Precursor Science (ADSPS) program under grant No. 80NSSC23K1476. C.K.H. acknowledges support from the National Science Foundation (NSF) Graduate Research Fellowship Program (GRFP) under Grant No. DGE 2146752. This research has made use of the NASA Exoplanet Archive, which is operated by the California Institute of Technology, under contract with the National Aeronautics and Space Administration under the Exoplanet Exploration Program. This research has also made use of the Habitable Zone Gallery at hzgallery.org. The results reported herein benefited from collaborations and/or information exchange within NASA's Nexus for Exoplanet System Science (NExSS) research coordination network sponsored by NASA's Science Mission Directorate.

Software: REBOUND (Rein & Liu 2012)

REFERENCES

- Akeson, R. L., Chen, X., Ciardi, D., et al. 2013, *PASP*, 125, 989, doi: [10.1086/672273](https://doi.org/10.1086/672273)
- Albrow, M. D., An, J., Beaulieu, J. P., et al. 2001, *ApJL*, 556, L113, doi: [10.1086/323141](https://doi.org/10.1086/323141)
- Alonso-Floriano, F. J., Morales, J. C., Caballero, J. A., et al. 2015, *A&A*, 577, A128, doi: [10.1051/0004-6361/201525803](https://doi.org/10.1051/0004-6361/201525803)
- Anglada-Escudé, G., López-Morales, M., & Chambers, J. E. 2010, *ApJ*, 709, 168, doi: [10.1088/0004-637X/709/1/168](https://doi.org/10.1088/0004-637X/709/1/168)
- Baker, V. R. 2001, *Nature*, 412, 228, doi: [10.1038/35084172](https://doi.org/10.1038/35084172)
- Barclay, T., Pepper, J., & Quintana, E. V. 2018, *ApJS*, 239, 2, doi: [10.3847/1538-4365/aae3e9](https://doi.org/10.3847/1538-4365/aae3e9)
- Barclay, T., Quintana, E. V., Raymond, S. N., & Penny, M. T. 2017, *ApJ*, 841, 86, doi: [10.3847/1538-4357/aa705b](https://doi.org/10.3847/1538-4357/aa705b)

- Barnes, R., & Raymond, S. N. 2004, *ApJ*, 617, 569, doi: [10.1086/423419](https://doi.org/10.1086/423419)
- Benedict, G. F., McArthur, B. E., Nelan, E. P., et al. 2022, *AJ*, 163, 295, doi: [10.3847/1538-3881/ac6ac8](https://doi.org/10.3847/1538-3881/ac6ac8)
- Bond, H. E., Bergeron, P., & Bédard, A. 2017, *ApJ*, 848, 16, doi: [10.3847/1538-4357/aa8a63](https://doi.org/10.3847/1538-4357/aa8a63)
- Bonomo, A. S., Dumusque, X., Massa, A., et al. 2023, *A&A*, 677, A33, doi: [10.1051/0004-6361/202346211](https://doi.org/10.1051/0004-6361/202346211)
- Bourrier, V., Dumusque, X., Dorn, C., et al. 2018, *A&A*, 619, A1, doi: [10.1051/0004-6361/201833154](https://doi.org/10.1051/0004-6361/201833154)
- Brewer, J. M., Fischer, D. A., Blackman, R. T., et al. 2020, *AJ*, 160, 67, doi: [10.3847/1538-3881/ab99c9](https://doi.org/10.3847/1538-3881/ab99c9)
- Brewer, J. M., Zhao, L. L., Fischer, D. A., et al. 2023, *AJ*, 166, 46, doi: [10.3847/1538-3881/acdd6f](https://doi.org/10.3847/1538-3881/acdd6f)
- Brown, R. A. 2015, *ApJ*, 799, 87, doi: [10.1088/0004-637X/799/1/87](https://doi.org/10.1088/0004-637X/799/1/87)
- Burrows, A., Halverson, S., Siegel, J. C., et al. 2024, *AJ*, 167, 243, doi: [10.3847/1538-3881/ad34d5](https://doi.org/10.3847/1538-3881/ad34d5)
- Carrera, D., Raymond, S. N., & Davies, M. B. 2019, *A&A*, 629, L7, doi: [10.1051/0004-6361/201935744](https://doi.org/10.1051/0004-6361/201935744)
- Cumming, A. 2004, *MNRAS*, 354, 1165, doi: [10.1111/j.1365-2966.2004.08275.x](https://doi.org/10.1111/j.1365-2966.2004.08275.x)
- Cumming, A., Butler, R. P., Marcy, G. W., et al. 2008, *PASP*, 120, 531, doi: [10.1086/588487](https://doi.org/10.1086/588487)
- Delrez, L., Ehrenreich, D., Alibert, Y., et al. 2021, *Nature Astronomy*, 5, 775, doi: [10.1038/s41550-021-01381-5](https://doi.org/10.1038/s41550-021-01381-5)
- Demory, B. O., Gillon, M., Deming, D., et al. 2011, *A&A*, 533, A114, doi: [10.1051/0004-6361/201117178](https://doi.org/10.1051/0004-6361/201117178)
- Dvorak, R., Pilat-Lohinger, E., Funk, B., & Freistetter, F. 2003, *A&A*, 410, L13, doi: [10.1051/0004-6361:20031404](https://doi.org/10.1051/0004-6361:20031404)
- Dvorak, R., Pilat-Lohinger, E., Bois, E., et al. 2010, *Astrobiology*, 10, 33, doi: [10.1089/ast.2009.0379](https://doi.org/10.1089/ast.2009.0379)
- Feng, F., Anglada-Escudé, G., Tuomi, M., et al. 2019, *MNRAS*, 490, 5002, doi: [10.1093/mnras/stz2912](https://doi.org/10.1093/mnras/stz2912)
- Feng, F., Tuomi, M., & Jones, H. R. A. 2017a, *A&A*, 605, A103, doi: [10.1051/0004-6361/201730406](https://doi.org/10.1051/0004-6361/201730406)
- Feng, F., Tuomi, M., Jones, H. R. A., et al. 2017b, *AJ*, 154, 135, doi: [10.3847/1538-3881/aa83b4](https://doi.org/10.3847/1538-3881/aa83b4)
- Feng, F., Butler, R. P., Jones, H. R. A., et al. 2021, *MNRAS*, 507, 2856, doi: [10.1093/mnras/stab2225](https://doi.org/10.1093/mnras/stab2225)
- Feng, F., Butler, R. P., Vogt, S. S., et al. 2022, *ApJS*, 262, 21, doi: [10.3847/1538-4365/ac7e57](https://doi.org/10.3847/1538-4365/ac7e57)
- Fischer, D. A., Anglada-Escudé, G., Arriagada, P., et al. 2016, *PASP*, 128, 066001, doi: [10.1088/1538-3873/128/964/066001](https://doi.org/10.1088/1538-3873/128/964/066001)
- Ford, E. B. 2005, *AJ*, 129, 1706, doi: [10.1086/427962](https://doi.org/10.1086/427962)
- . 2008, *AJ*, 135, 1008, doi: [10.1088/0004-6256/135/3/1008](https://doi.org/10.1088/0004-6256/135/3/1008)
- . 2014, *Proceedings of the National Academy of Science*, 111, 12616, doi: [10.1073/pnas.1304219111](https://doi.org/10.1073/pnas.1304219111)
- Fulton, B. J., Rosenthal, L. J., Hirsch, L. A., et al. 2021, *ApJS*, 255, 14, doi: [10.3847/1538-4365/abfcc1](https://doi.org/10.3847/1538-4365/abfcc1)
- Gaia Collaboration, Brown, A. G. A., Vallenari, A., et al. 2021, *A&A*, 649, A1, doi: [10.1051/0004-6361/202039657](https://doi.org/10.1051/0004-6361/202039657)
- Galland, F., Lagrange, A. M., Udry, S., et al. 2005, *A&A*, 444, L21, doi: [10.1051/0004-6361:200500176](https://doi.org/10.1051/0004-6361:200500176)
- Gillon, M., Demory, B.-O., Van Grootel, V., et al. 2017, *Nature Astronomy*, 1, 0056, doi: [10.1038/s41550-017-0056](https://doi.org/10.1038/s41550-017-0056)
- Goździewski, K., Bois, E., Maciejewski, A. J., & Kiseleva-Eggleton, L. 2001, *A&A*, 378, 569, doi: [10.1051/0004-6361:20011189](https://doi.org/10.1051/0004-6361:20011189)
- Gregory, P. C., & Fischer, D. A. 2010, *MNRAS*, 403, 731, doi: [10.1111/j.1365-2966.2009.16233.x](https://doi.org/10.1111/j.1365-2966.2009.16233.x)
- Hadden, S. 2019, *AJ*, 158, 238, doi: [10.3847/1538-3881/ab5287](https://doi.org/10.3847/1538-3881/ab5287)
- Hara, N. C., Boué, G., Laskar, J., Delisle, J. B., & Unger, N. 2019, *MNRAS*, 489, 738, doi: [10.1093/mnras/stz1849](https://doi.org/10.1093/mnras/stz1849)
- Harada, C. K., Dressing, C. D., Kane, S. R., & Ardestani, B. A. 2024, *ApJS*, 272, 30, doi: [10.3847/1538-4365/ad3e81](https://doi.org/10.3847/1538-4365/ad3e81)
- Hatzes, A. P., Gandolfi, D., Korth, J., et al. 2022, *AJ*, 163, 223, doi: [10.3847/1538-3881/ac5dcb](https://doi.org/10.3847/1538-3881/ac5dcb)
- He, M. Y., Ford, E. B., & Ragozzine, D. 2019, *MNRAS*, 490, 4575, doi: [10.1093/mnras/stz2869](https://doi.org/10.1093/mnras/stz2869)
- Hill, M. L., Bott, K., Dalba, P. A., et al. 2023, *AJ*, 165, 34, doi: [10.3847/1538-3881/aca1c0](https://doi.org/10.3847/1538-3881/aca1c0)
- Hill, M. L., Kane, S. R., Seperuelo Duarte, E., et al. 2018, *ApJ*, 860, 67, doi: [10.3847/1538-4357/aac384](https://doi.org/10.3847/1538-4357/aac384)
- Holman, M. J., & Wiegert, P. A. 1999, *AJ*, 117, 621, doi: [10.1086/300695](https://doi.org/10.1086/300695)
- Huang, C. X., Burt, J., Vanderburg, A., et al. 2018, *ApJL*, 868, L39, doi: [10.3847/2041-8213/aaef91](https://doi.org/10.3847/2041-8213/aaef91)
- Hurt, S. A., Fulton, B., Isaacson, H., et al. 2022, *AJ*, 163, 218, doi: [10.3847/1538-3881/ac5c47](https://doi.org/10.3847/1538-3881/ac5c47)
- Jeffers, S. V., Dreizler, S., Barnes, J. R., et al. 2020, *Science*, 368, 1477, doi: [10.1126/science.aaz0795](https://doi.org/10.1126/science.aaz0795)
- Kane, S. R. 2014, *ApJ*, 782, 111, doi: [10.1088/0004-637X/782/2/111](https://doi.org/10.1088/0004-637X/782/2/111)
- . 2015, *ApJL*, 814, L9, doi: [10.1088/2041-8205/814/1/L9](https://doi.org/10.1088/2041-8205/814/1/L9)
- . 2016, *ApJ*, 830, 105, doi: [10.3847/0004-637X/830/2/105](https://doi.org/10.3847/0004-637X/830/2/105)
- . 2023, *AJ*, 166, 187, doi: [10.3847/1538-3881/acfb01](https://doi.org/10.3847/1538-3881/acfb01)
- Kane, S. R., & Blunt, S. 2019, *AJ*, 158, 209, doi: [10.3847/1538-3881/ab4c3e](https://doi.org/10.3847/1538-3881/ab4c3e)
- Kane, S. R., & Byrne, P. K. 2024, *Nature Astronomy*, 8, 417, doi: [10.1038/s41550-024-02228-5](https://doi.org/10.1038/s41550-024-02228-5)
- Kane, S. R., Ciardi, D. R., Gelino, D. M., & von Braun, K. 2012, *MNRAS*, 425, 757, doi: [10.1111/j.1365-2966.2012.21627.x](https://doi.org/10.1111/j.1365-2966.2012.21627.x)
- Kane, S. R., & Fetherolf, T. 2023, *AJ*, 166, 205, doi: [10.3847/1538-3881/acff5a](https://doi.org/10.3847/1538-3881/acff5a)

- Kane, S. R., & Gelino, D. M. 2012, *PASP*, 124, 323, doi: [10.1086/665271](https://doi.org/10.1086/665271)
- Kane, S. R., Gelino, D. M., Ciardi, D. R., Dragomir, D., & von Braun, K. 2011, *ApJ*, 740, 61, doi: [10.1088/0004-637X/740/2/61](https://doi.org/10.1088/0004-637X/740/2/61)
- Kane, S. R., & Hinkel, N. R. 2013, *ApJ*, 762, 7, doi: [10.1088/0004-637X/762/1/7](https://doi.org/10.1088/0004-637X/762/1/7)
- Kane, S. R., Kopparapu, R. K., & Domagal-Goldman, S. D. 2014, *ApJL*, 794, L5, doi: [10.1088/2041-8205/794/1/L5](https://doi.org/10.1088/2041-8205/794/1/L5)
- Kane, S. R., Mahadevan, S., von Braun, K., Laughlin, G., & Ciardi, D. R. 2009, *PASP*, 121, 1386, doi: [10.1086/648564](https://doi.org/10.1086/648564)
- Kane, S. R., Meshkat, T., & Turnbull, M. C. 2018, *AJ*, 156, 267, doi: [10.3847/1538-3881/aac981](https://doi.org/10.3847/1538-3881/aac981)
- Kane, S. R., & Raymond, S. N. 2014, *ApJ*, 784, 104, doi: [10.1088/0004-637X/784/2/104](https://doi.org/10.1088/0004-637X/784/2/104)
- Kane, S. R., Schneider, D. P., & Ge, J. 2007, *MNRAS*, 377, 1610, doi: [10.1111/j.1365-2966.2007.11722.x](https://doi.org/10.1111/j.1365-2966.2007.11722.x)
- Kane, S. R., Turnbull, M. C., Fulton, B. J., et al. 2020a, *AJ*, 160, 81, doi: [10.3847/1538-3881/ab9ffe](https://doi.org/10.3847/1538-3881/ab9ffe)
- Kane, S. R., & von Braun, K. 2008, *ApJ*, 689, 492, doi: [10.1086/592381](https://doi.org/10.1086/592381)
- Kane, S. R., & Wittenmyer, R. A. 2024, *ApJL*, 962, L21, doi: [10.3847/2041-8213/ad2463](https://doi.org/10.3847/2041-8213/ad2463)
- Kane, S. R., Hill, M. L., Kasting, J. F., et al. 2016, *ApJ*, 830, 1, doi: [10.3847/0004-637X/830/1/1](https://doi.org/10.3847/0004-637X/830/1/1)
- Kane, S. R., Arney, G., Crisp, D., et al. 2019, *Journal of Geophysical Research (Planets)*, 124, 2015, doi: [10.1029/2019JE005939](https://doi.org/10.1029/2019JE005939)
- Kane, S. R., Yalçınkaya, S., Osborn, H. P., et al. 2020b, *AJ*, 160, 129, doi: [10.3847/1538-3881/aba835](https://doi.org/10.3847/1538-3881/aba835)
- Kasting, J. F., Whitmire, D. P., & Reynolds, R. T. 1993, *Icarus*, 101, 108, doi: [10.1006/icar.1993.1010](https://doi.org/10.1006/icar.1993.1010)
- King, R. R., McCaughrean, M. J., Homeier, D., et al. 2010, *A&A*, 510, A99, doi: [10.1051/0004-6361/200912981](https://doi.org/10.1051/0004-6361/200912981)
- Kipping, D. M., & Sandford, E. 2016, *MNRAS*, 463, 1323, doi: [10.1093/mnras/stw1926](https://doi.org/10.1093/mnras/stw1926)
- Kopparapu, R. K., & Barnes, R. 2010, *ApJ*, 716, 1336, doi: [10.1088/0004-637X/716/2/1336](https://doi.org/10.1088/0004-637X/716/2/1336)
- Kopparapu, R. K., Ramirez, R. M., SchottelKotte, J., et al. 2014, *ApJ*, 787, L29, doi: [10.1088/2041-8205/787/2/L29](https://doi.org/10.1088/2041-8205/787/2/L29)
- Kopparapu, R. K., Ramirez, R., Kasting, J. F., et al. 2013, *ApJ*, 765, 131, doi: [10.1088/0004-637X/765/2/131](https://doi.org/10.1088/0004-637X/765/2/131)
- Kopparapu, R. K., Hébrard, E., Belikov, R., et al. 2018, *ApJ*, 856, 122, doi: [10.3847/1538-4357/aab205](https://doi.org/10.3847/1538-4357/aab205)
- Li, Z., Hildebrandt, S. R., Kane, S. R., et al. 2021, *AJ*, 162, 9, doi: [10.3847/1538-3881/abf831](https://doi.org/10.3847/1538-3881/abf831)
- Lovis, C., Mayor, M., Pepe, F., et al. 2006, *Nature*, 441, 305, doi: [10.1038/nature04828](https://doi.org/10.1038/nature04828)
- Luhman, K. L., Patten, B. M., Marengo, M., et al. 2007, *ApJ*, 654, 570, doi: [10.1086/509073](https://doi.org/10.1086/509073)
- Luhn, J. K., Bastien, F. A., Wright, J. T., et al. 2019, *AJ*, 157, 149, doi: [10.3847/1538-3881/aaf5d0](https://doi.org/10.3847/1538-3881/aaf5d0)
- Ma, B., Ge, J., Muterspaugh, M., et al. 2018, *MNRAS*, 480, 2411, doi: [10.1093/mnras/sty1933](https://doi.org/10.1093/mnras/sty1933)
- Mamajek, E., & Stapelfeldt, K. 2024, arXiv e-prints, arXiv:2402.12414, doi: [10.48550/arXiv.2402.12414](https://doi.org/10.48550/arXiv.2402.12414)
- Marcy, G. W., Butler, R. P., Fischer, D. A., et al. 2002, *ApJ*, 581, 1375, doi: [10.1086/344298](https://doi.org/10.1086/344298)
- Marmier, M., Ségransan, D., Udry, S., et al. 2013, *A&A*, 551, A90, doi: [10.1051/0004-6361/201219639](https://doi.org/10.1051/0004-6361/201219639)
- Mason, B. D., Wycoff, G. L., Hartkopf, W. I., Douglass, G. G., & Worley, C. E. 2001, *AJ*, 122, 3466, doi: [10.1086/323920](https://doi.org/10.1086/323920)
- Mayor, M., Udry, S., Naef, D., et al. 2004, *A&A*, 415, 391, doi: [10.1051/0004-6361:20034250](https://doi.org/10.1051/0004-6361:20034250)
- Menou, K., & Tabachnik, S. 2003, *ApJ*, 583, 473, doi: [10.1086/345359](https://doi.org/10.1086/345359)
- Naef, D., Mayor, M., Korzennik, S. G., et al. 2003, *A&A*, 410, 1051, doi: [10.1051/0004-6361:20031341](https://doi.org/10.1051/0004-6361:20031341)
- Orosei, R., Lauro, S. E., Pettinelli, E., et al. 2018, *Science*, 361, 490, doi: [10.1126/science.aar7268](https://doi.org/10.1126/science.aar7268)
- O'Toole, S. J., Tinney, C. G., Jones, H. R. A., et al. 2009, *MNRAS*, 392, 641, doi: [10.1111/j.1365-2966.2008.14051.x](https://doi.org/10.1111/j.1365-2966.2008.14051.x)
- Pepe, F., Lovis, C., Ségransan, D., et al. 2011, *A&A*, 534, A58, doi: [10.1051/0004-6361/201117055](https://doi.org/10.1051/0004-6361/201117055)
- Petrovich, C., Malhotra, R., & Tremaine, S. 2013, *ApJ*, 770, 24, doi: [10.1088/0004-637X/770/1/24](https://doi.org/10.1088/0004-637X/770/1/24)
- Porto de Mello, G. F., & da Silva, L. 1997, *ApJL*, 476, L89, doi: [10.1086/310504](https://doi.org/10.1086/310504)
- Raghavan, D., McAlister, H. A., Henry, T. J., et al. 2010, *ApJS*, 190, 1, doi: [10.1088/0067-0049/190/1/1](https://doi.org/10.1088/0067-0049/190/1/1)
- Raymond, S. N., Barnes, R., Armitage, P. J., & Gorelick, N. 2008, *ApJL*, 687, L107, doi: [10.1086/593301](https://doi.org/10.1086/593301)
- Raymond, S. N., & Bonsor, A. 2014, *MNRAS*, 442, L18, doi: [10.1093/mnras/1slu048](https://doi.org/10.1093/mnras/1slu048)
- Raymond, S. N., & Izidoro, A. 2017, *Icarus*, 297, 134, doi: [10.1016/j.icarus.2017.06.030](https://doi.org/10.1016/j.icarus.2017.06.030)
- Rein, H., & Liu, S. F. 2012, *A&A*, 537, A128, doi: [10.1051/0004-6361/201118085](https://doi.org/10.1051/0004-6361/201118085)
- Rein, H., & Tamayo, D. 2015, *MNRAS*, 452, 376, doi: [10.1093/mnras/stv1257](https://doi.org/10.1093/mnras/stv1257)
- Rosenthal, L. J., Fulton, B. J., Hirsch, L. A., et al. 2021, *ApJS*, 255, 8, doi: [10.3847/1538-4365/abe23c](https://doi.org/10.3847/1538-4365/abe23c)
- Scholz, R. D., McCaughrean, M. J., Lodieu, N., & Kuhlbrodt, B. 2003, *A&A*, 398, L29, doi: [10.1051/0004-6361:20021847](https://doi.org/10.1051/0004-6361:20021847)
- Shen, Y., & Turner, E. L. 2008, *ApJ*, 685, 553, doi: [10.1086/590548](https://doi.org/10.1086/590548)
- Simonetti, P., Vladilo, G., Silva, L., & Sozzetti, A. 2020, *ApJ*, 903, 141, doi: [10.3847/1538-4357/abc074](https://doi.org/10.3847/1538-4357/abc074)

- Stark, C. C., Dressing, C., Dulz, S., et al. 2020, *AJ*, 159, 286, doi: [10.3847/1538-3881/ab8f26](https://doi.org/10.3847/1538-3881/ab8f26)
- Stark, C. C., Latouf, N., Mandell, A. M., & Young, A. 2024, *Journal of Astronomical Telescopes, Instruments, and Systems*, 10, 014005, doi: [10.1117/1.JATIS.10.1.014005](https://doi.org/10.1117/1.JATIS.10.1.014005)
- Stassun, K. G., Collins, K. A., & Gaudi, B. S. 2017, *AJ*, 153, 136, doi: [10.3847/1538-3881/aa5df3](https://doi.org/10.3847/1538-3881/aa5df3)
- Tinney, C. G., Butler, R. P., Jones, H. R. A., et al. 2011, *ApJ*, 727, 103, doi: [10.1088/0004-637X/727/2/103](https://doi.org/10.1088/0004-637X/727/2/103)
- Tuchow, N. W., Stark, C. C., & Mamajek, E. 2024, *AJ*, 167, 139, doi: [10.3847/1538-3881/ad25ec](https://doi.org/10.3847/1538-3881/ad25ec)
- Unger, N., Ségransan, D., Queloz, D., et al. 2021, *A&A*, 654, A104, doi: [10.1051/0004-6361/202141351](https://doi.org/10.1051/0004-6361/202141351)
- Vaughan, S. R., Gebhard, T. D., Bott, K., et al. 2023, *MNRAS*, 524, 5477, doi: [10.1093/mnras/stad2127](https://doi.org/10.1093/mnras/stad2127)
- Venturini, J., Ronco, M. P., & Guilera, O. M. 2020, *SSRv*, 216, 86, doi: [10.1007/s11214-020-00700-y](https://doi.org/10.1007/s11214-020-00700-y)
- Vogt, S. S., Wittenmyer, R. A., Butler, R. P., et al. 2010, *ApJ*, 708, 1366, doi: [10.1088/0004-637X/708/2/1366](https://doi.org/10.1088/0004-637X/708/2/1366)
- Vogt, S. S., Burt, J., Meschiari, S., et al. 2015, *ApJ*, 814, 12, doi: [10.1088/0004-637X/814/1/12](https://doi.org/10.1088/0004-637X/814/1/12)
- von Braun, K., Kane, S. R., & Ciardi, D. R. 2009, *ApJ*, 702, 779, doi: [10.1088/0004-637X/702/1/779](https://doi.org/10.1088/0004-637X/702/1/779)
- von Braun, K., Boyajian, T. S., ten Brummelaar, T. A., et al. 2011, *ApJ*, 740, 49, doi: [10.1088/0004-637X/740/1/49](https://doi.org/10.1088/0004-637X/740/1/49)
- Way, M. J., Del Genio, A. D., Kiang, N. Y., et al. 2016, *Geophys. Res. Lett.*, 43, 8376, doi: [10.1002/2016GL069790](https://doi.org/10.1002/2016GL069790)
- Williams, J. G., & Benson, G. S. 1971, *AJ*, 76, 167, doi: [10.1086/111100](https://doi.org/10.1086/111100)
- Winn, J. N., & Fabrycky, D. C. 2015, *ARA&A*, 53, 409, doi: [10.1146/annurev-astro-082214-122246](https://doi.org/10.1146/annurev-astro-082214-122246)
- Winn, J. N., Matthews, J. M., Dawson, R. I., et al. 2011, *ApJL*, 737, L18, doi: [10.1088/2041-8205/737/1/L18](https://doi.org/10.1088/2041-8205/737/1/L18)
- Wittenmyer, R. A., Bergmann, C., Horner, J., Clark, J., & Kane, S. R. 2019a, *MNRAS*, 484, 4230, doi: [10.1093/mnras/stz236](https://doi.org/10.1093/mnras/stz236)
- Wittenmyer, R. A., Clark, J. T., Zhao, J., et al. 2019b, *MNRAS*, 484, 5859, doi: [10.1093/mnras/stz290](https://doi.org/10.1093/mnras/stz290)
- Wittenmyer, R. A., Tinney, C. G., O’Toole, S. J., et al. 2011, *ApJ*, 727, 102, doi: [10.1088/0004-637X/727/2/102](https://doi.org/10.1088/0004-637X/727/2/102)
- Wittenmyer, R. A., Tinney, C. G., Horner, J., et al. 2013, *PASP*, 125, 351, doi: [10.1086/670680](https://doi.org/10.1086/670680)
- Wittenmyer, R. A., Butler, R. P., Tinney, C. G., et al. 2016, *ApJ*, 819, 28, doi: [10.3847/0004-637X/819/1/28](https://doi.org/10.3847/0004-637X/819/1/28)
- Wittenmyer, R. A., Wang, S., Horner, J., et al. 2020, *MNRAS*, 492, 377, doi: [10.1093/mnras/stz3436](https://doi.org/10.1093/mnras/stz3436)
- Xuan, J. W., & Wyatt, M. C. 2020, *MNRAS*, 497, 2096, doi: [10.1093/mnras/staa2033](https://doi.org/10.1093/mnras/staa2033)
- Zakamska, N. L., Pan, M., & Ford, E. B. 2011, *MNRAS*, 410, 1895, doi: [10.1111/j.1365-2966.2010.17570.x](https://doi.org/10.1111/j.1365-2966.2010.17570.x)